

The ISOLDE RILIS pump laser upgrade and the LARIS Laboratory

**B.A. Marsh, L.-E Berg¹, D.V. Fedorov², V.N. Fedosseev, O.J. Launila¹
M. Lindroos, R. Losito, F.K. Österdahl¹, T. Pauchard¹,
I.T. Pohjalainen³, U. Sassenberg⁴, M.D. Seliverstov²,
A.M. Sjödin, G. Tranströmer¹**

Abstract

On account of its high efficiency, speed and unmatched selectivity, the Resonance Ionization Laser Ion Source (RILIS) is the preferred method for ionizing the nuclear reaction products at the ISOLDE on-line isotope separator facility. By exploiting the unique electronic energy level 'fingerprint' of a chosen element, the RILIS process of laser step-wise resonance ionization enables an ion beam of high chemical purity to be sent through the mass selective separator magnet. The isobaric purity of a beam of a chosen isotope is therefore greatly increased. The RILIS, comprising of up to three frequency tunable pulsed dye lasers has been upgraded with the installation of a Nd:YAG pump laser as a replacement for the old Copper Vapor Laser (CVL) system. A summary of the current Nd:YAG pumped RILIS performance is given. To accompany the RILIS pump laser upgrade, a new ionization scheme for manganese has been developed at the newly constructed LASer Resonance Ionization Spectroscopy (LARIS) laboratory and successfully applied for on-line RILIS operation. An overview of the LARIS facility is given along with details of the ionization scheme development work for manganese.

1 KTH-Royal Institute of Technology, SE-10044 Stockholm, Sweden
2 Petersburg Nuclear Physics Institute, 188350 Gatchina, Russia
3 Accelerator Laboratory, University of Jyväskylä, SF 403 51 Jyväskylä, Finland
4 Fysikum, Stockholm University, SE-10691 Stockholm, Sweden



1 Introduction

The ISOLDE facility produces radioactive isotopes using the Isotope Separator On Line (ISOL) technique whereby a driver beam impinges upon a fixed target. The reaction products are ionized, extracted and then mass separated during their flight towards the experimental setup. The success of such a technique hinges on the ability to couple high production rates of a wide range of isotopes with their fast, efficient and selective extraction. At ISOLDE the pulsed driver beam of the 1.4 GeV CERN PS booster synchrotron, containing up to 3×10^{13} protons per bunch, is incident upon a thick target (typically >10 g/cm² uranium carbide). The products from fission, spallation and fragmentation reactions are stopped and neutralized within the target matrix and then rely on diffusion and effusion to reach the ionization region. Ionization enables electrostatic acceleration and subsequent isotope selection by mass separation in a bending magnet. Due to the presence of multiple isobars at a chosen mass, unambiguous isotope selection cannot be guaranteed by mass separation alone. The Resonance Ionization Laser Ion Source (RILIS) [1], [2] addresses this by ensuring that the element of interest is preferentially ionized. The isobaric purity of the beam is therefore greatly improved prior to its passage through the mass separator. The RILIS is a system of pulsed laser beams that interact with the atomic vapor as it exits the target. Each laser is precisely tuned so that the photon energies match the unique combination of successive electronic transition energies within an ionization scheme for a chosen element. The excited atom is then ionized by a final resonant or non resonant photon absorption step. Currently the RILIS is capable of ionizing 28 of the elements that are released from the ISOLDE target. On account of the high degree of selectivity offered for these elements, RILIS operation is requested for over 50% of the ISOLDE beam-time. In line with the planning of the HIE-ISOLDE project [3], the RILIS system has undergone the first phase of an upgrade program with the installation of a new Nd:YAG laser as a replacement for the aging Copper Vapor Laser (CVL) system. This has been completed in conjunction with the construction of a new off-line spectroscopy laboratory (LARIS) designed for the study of ionization schemes for stable isotopes by means of resonance ionization spectroscopy, and technical development work to enhance RILIS efficiency, selectivity and applicability. The necessity of the LARIS lab is exemplified by the need for a new ionization scheme for manganese due to the incompatibility of the new Nd:YAG based RILIS system with the previously used scheme. These details are discussed in Section 3 along with the some results of a spectroscopy study performed at the LARIS laboratory in which many new ionization schemes for manganese were measured.

2 RILIS pump laser upgrade

A detailed description of the CVL based RILIS system is given in [2] and the justification for the replacement of the CVL system with a solid state laser is given in [4] along with the performance requirements for the new laser. The RILIS has been operating at ISOLDE for on-line physics runs since 1994 using a CVL system of three laser tubes operating in Master Oscillator - Power Amplifier (MOPA) mode supplying the pump power for up to three dye lasers as well as a low divergence beam for direct injection to the ionizer cavity. Aside from some modernization of the laser tubes and the power supply, the system remained essentially unchanged, even as the demand for RILIS beams increased to over 2000 hours annually. To reliably meet this increasing demand for RILIS operation and to improve the stability and overall performance of the system, the replacement of the CVL with a commercially available solid state laser was deemed necessary. A market survey revealed only one company, *EdgeWave GmbH* (Würselen, Germany), with a proven ability to produce a laser close to the desired specification. The greatest constraint was the need for high output power (80 W at 532 nm), high repetition rate (10 kHz) and short pulse length (<15 ns): a combination atypical of commercially available Nd:YAG lasers which often have pulse lengths in excess of 100 ns. The *INNOSLAB* concept [5] developed by *EdgeWave* addresses this by using an end-pumped YAG slab within a small resonator cavity. The *EdgeWave* laser was ordered in July 2007, installed alongside the CVL system and tested during the 2007/2008 ISOLDE off-line period. Table 1 gives an overview of the maximum CVL performance, the Nd:YAG performance requirements

Table 1: RILIS pump laser parameters. The desired values for the pump laser upgrade taken from [4] and the measured values for the *EdgeWave* laser are given

Parameter	CVL		Nd:YAG			Nd:YAG (<i>measured</i>)		
	Green	Yellow	Beam A	Beam B	Beam C	Beam A	Beam B	Beam C
Wavelength, nm	511	578	532	532	355	532	532	355
Repetition rate, kHz	11	11	8-15	8-15	8-15	10	10	10
Average power, W	45	35	40	30-40	15-20	75	15 (28 [†])	20
Pulse duration, ns	15	15	10-30	10-20	10-20	8	9	11
Timing jitter, ns	4-8	4-8	<3	<3	<3	<3	<3	<3
Transmission to cavity	25%	25%	not specified			32%	N/A	N/A

[†]The power output of the 2nd green beam is dependent on the optimization of the temperature controlled phase matching for the UV generation crystal. In normal operation UV power is minimized and this value is achievable.

detailed in [4], and the measured performance of the new laser.

Whilst the total green and UV power demands have been met by the *EdgeWave* laser, the distribution of the power between beam A and beam B differ from those of the desired laser specifications. This is due to a change from the originally foreseen solution of having three separate lasers to provide beams A, B and C. Beam A is intended for use as the ionizing laser for schemes relying on a non-resonant final step and so has a strict maximum acceptable divergence of 0.1 mrad and a beam pointing stability of 0.02 mrad to ensure good transmission and focusing in the 3 mm ion source cavity, situated at a distance of up to 23 m. Beams B and C are to be used only for dye laser pumping and so these values can increase by an order of magnitude without significant performance degradation. For the *EdgeWave* laser, beams A, B and C originate from a single laser which produces a fundamental beam of 160 W. This beam enters a Lithium Triborate (LBO) crystal for frequency doubling to produce the primary green beam (beam A), which is separated from the residual fundamental beam and sent through a dedicated output port of the laser head. The residual fundamental beam enters a doubling and tripling unit containing two LBO crystals. Within the laser head a beamsplitter picks off the third harmonic (beam C) to direct it through a second output port. The residual fundamental beam and the second harmonic (beam B) exit the laser head together through a third port and are separated externally. This solution results in an uneven distribution of green power between beam A and beam B but is favorable in that it does not limit the maximum power that is available for direct transmission to the ion source to 40 W. An important advantage of this solution is the absence of timing jitter between the pulses of beams A, B and C.

2.1 Nd:YAG vs CVL operation

The installation of the new pump laser was completed before the summer on-line period of 2008 with the intention of fulfilling the 2008 demand for RILIS beams using either CVL or Nd:YAG pumping. In its first year of operation the Nd:YAG laser was used for 61% (1231 hours) of the RILIS on-line operation. The CVL system remained in place throughout the 2009 on-line period but was not required and the new pump laser was operational for 100% of the requested RILIS beamtime.

The complete transition from CVL to Nd:YAG pumping necessitates adaptations to the established ionization scheme and/or laser setup for several RILIS elements. This is due to fundamental differences between the laser beam characteristics. The factors that are known to or could be expected to influence the performance of an existing RILIS scheme when using the new pump laser are described below and the affected ionization schemes are listed.

Table 2: Ionization schemes used at the ISOLDE RILIS: IP - ionization potential; $\lambda_1, \lambda_2, \lambda_3$ - wavelengths (air) of the first, second and third excitation transitions; P_1, P_2, P_3 , - power values of laser beams injected into the RILIS cavity; η_{ion} - ionization efficiency. The data are taken from [4] with the new values for the Nd:YAG pumped schemes added in **bold type**

Element	IP,eV	λ_1 ,nm	P_1 ,mW	λ_2 ,nm	P_2 ,mW	λ_3 ,nm	P_3 ,mW	$\eta_{ion},\%$
^4Be	9.32	234.86	20	297.32	300	-	-	>7
		234.86	20	297.32	300	-	-	
^{12}Mg	7.65	285.21	40	552.84	80	511, 578	5000	10
		285.21	50	552.84	140	532	13500	
^{13}Al	5.99	309.27	50	511, 578	5000	-	-	>20
^{21}Sc	6.56	327.36	20	719.83	60	511, 578	-	15
^{20}Ca	6.11	272.16	100	511, 578	5000	-	-	0.45
^{25}Mn	7.44	279.83	50	628.27	1200	511	3000	19
		279.83	50	628.27	1200	647.34	625	
^{27}Co	7.88	304.40	120	544.46	150	511, 578	5000	>4
^{28}Ni	7.64	305.08	60	611.11	250	748.22	1200	>6
		305.08	50	611.11	275	748.22	1000	
^{29}Cu	7.73	327.40	50	287.89	250	-	-	>7
		327.40	25	287.89	250	-	-	
^{30}Zn	9.39	213.86	20	636.23	150	511	3000	5
		213.86	5	636.23	500	532	7000	
^{31}Ga	6.00	287.42	70	511	5000	-	-	21
		287.42	50	532	10000	-	-	
Simultaneously {		294.36	50					
^{39}Y	6.22	408.37	100	581.91	1900	581.91	1900	-
^{47}Ag	7.58	328.07	70	546.55	100	511, 578	5000	14
^{48}Cd	8.99	228.80	20	643.85	300	511	3000	10
^{49}In	6.00	303.94	50	511, 578	5000	-	-	-
^{50}Sn	7.34	300.91	50	811.40	100	823.49	500	≈ 9
		300.91	50	811.40	150	823.49	1100	
^{51}Sb	8.61	217.58	12	560.21	150	511	6000	2.7
^{60}Nd	5.53	588.79	700	596.94	4500	596.94	4500	
^{65}Tb	5.86	579.56	300	551.65	200	618.25	1200	-
^{66}Dy	5.94	625.91	170	607.50	90	511	3500	20
^{70}Yb	6.25	555.65	200	581.03	1200	581.03	1200	-
^{79}Au	9.23	267.59	80	306.54	40	673.9	370	>3
^{80}Hg	10.44	253.65	8	313.18	100	626.3	1200	0.1
^{81}Tl	6.11	276.79	70	511, 578	5000	-	-	27
		276.79	100	532	15000	-	-	
^{82}Pb	7.42	283.30	70	600.19	500	511, 578	5000	3
^{83}Bi	7.29	306.77	50	555.20	500	511, 578	-	6
^{84}Po	8.42	255.80	20	843.38	500	511	3000	>0.4
		255.80	20	843.38	150	532	7500	

2.1.0.1 Wavelength difference

The small change in the main pump beam wavelength (532 nm instead of 511 and 578 nm) can influence the performance or feasibility of an ionization scheme in several ways.

- The lower limit of wavelength of the 532 nm pumped dye laser output is shifted from 520 to 543 nm:
Ca, Au.
- Differing 532 nm, 511 nm and 578 nm pump beam absorption rates for laser dyes:
Be, Ca, Ni, Mn, Sc, Po.
- Any difference in photon absorption cross section at the pump beam wavelength for ionization schemes using the Nd:YAG or CVL beam for the final step:
Mn, Pb.

An advantage of the Nd:YAG laser is the availability of a 355 nm beam which is intended for the pumping of laser dyes that emit light in the 372 - 550 nm range. This capability has been tested for 7 of the dyes within this range. An upgrade or replacement of one of the dye lasers is necessary to enable full use of UV pumping since the RILIS dye lasers are optimized for CVL pumped dyes and the efficiency reduces below 520 nm due to increased cavity losses.

2.1.0.2 Shorter pulse length

As well as influencing the dye laser efficiency, the shorter pulse length of the Nd:YAG laser results in a lower pulse energy damage threshold for the Beta-Barium Borate (BBO) crystals used for multiple harmonic generation. This is particularly apparent for generation of third harmonics at wavelengths below 225 nm, where the photon absorption in BBO becomes significant: *Zn, Sb.*

2.1.0.3 Beam focusing in the ion source

The unstable resonator configuration of the CVL oscillator cavity results in a low divergence beam which is capable of producing a focal point of less than 5 mm in diameter at the distance of approximately 25 m to the HRS ion source cavity. This is essential for the current ionization schemes of the 17 RILIS elements which rely on non resonant ionization using the pump laser beam. Since these ionization steps cannot be saturated with the available laser power, any improvement in the laser beam transport efficiency to the ion source results in a proportional increase in the ionization efficiency. As shown in the final row of Table 1, the efficiency of the Nd:YAG laser beam transport to the ion source is slightly greater than can be achieved with CVL system. It has been observed that, unlike the CVL beam which comprises of a single beam with a flat-top profile, beam A of the Nd:YAG laser has a central Gaussian profile (60 % of the total power) but contains two or more satellite components. These satellites are lost within the telescope system used for focusing the central component at the ion source. The possibility of improving the composition of beam A, to increase the proportion of the beam within the central component is being discussed with the laser manufacturer: *Mg, Al, Ca, Sc, Co, Zn, Ga, Y, Ag, Cd, In, Sb, Dy, Tl, Pb, Bi, Po.*

2.1.0.4 Reliability

Because of the high intensity of RILIS operation during a typical annual experimental period the reliability of the pump laser is of prime importance. In 2009, RILIS beams were used for 250 shifts spread over 14 experiments studying 10 different elements (Be, Ga, Ag, Nd, Po, Mn, Mg, Sn, Zn and Ni). This equated to a total of 2142 hours of Nd:YAG laser operation. This operation performed by the CVL system would typically require a considerable amount of maintenance in the form of either scheduled replacement of components or unanticipated repair work. The replacement of the homemade CVL with the commercial Nd:YAG system has greatly reduced the frequency of required interventions. However, with the exception of the cooling and dehumidifying system, the Nd:YAG components are inaccessible

and the user controlled parameters are adjustable only via the factory recommended remote control interfaces. Any non-trivial work can therefore no longer be carried out on-site and the laser must be shipped back to the manufacturer. In order for this new mode of operation to be feasible it is necessary to have a complete replacement system (laser, power supply and chiller unit), ready for immediate installation in the event of a laser failure during an experimental run.

Table 2 gives an overview of the current RILIS operating parameters including details of the Nd:YAG pumped dye laser performance for schemes that so far been used on-line. The RILIS performance for Mg, Zn, Sn, Tl, and Po ionization has improved simply due to the increase in power available for the non-resonant ionization step. For gallium, the extra green power was instead used for pumping a second dye laser. The frequency doubled output of this laser was used for the excitation of gallium atoms from a thermally populated ($\approx 50\%$ at 2000°C) level at 826.24 cm^{-1} . By simultaneously exciting from the ground-state and the thermally populated level, the ionization efficiency is approximately doubled.

3 The LARIS Laboratory

Prior to the existence of the LARIS laboratory, ionization scheme development for RILIS has been performed off-line at the ISOLDE facility. This procedure, as described in [6] requires dedicated use of one of the two ISOLDE mass separators and a target unit loaded with two samples of the element being studied. A large sample provides a reliable long term source of atoms for ionization scheme investigations and a smaller, independently controlled and carefully measured sample of typically 2000 nAh is used for an efficiency measurement of the optimal ionization scheme. Depending on the complexity of the ionization scheme, the availability of data on the atomic spectrum or previously used ionization schemes, such a study can take between 3 to 10 days per element. Often, due to time constraints, the scope for scheme development for a particular element is limited to testing resonant transitions between well documented atomic levels and a non-resonant ionization step using the residual power of the the pump laser is used. This is unfortunate since the photon absorption cross section for a transition to an auto-ionization state can be several orders of magnitude greater, resulting in an increase in ionization efficiency despite the lower power of a tunable laser. The LARIS laboratory has been constructed as a versatile tool for ionization scheme development which is independent of the scheduling constraints of the ISOLDE work program, therefore enabling thorough ionization scheme studies to be performed. A system of three tunable lasers (Table 3) and two atomic beam chambers are available for performing resonance ionization spectroscopy studies. The principal scanning laser, a Spectra-Physics MOPO-HF is an all solid state system capable of performing a continuous scan from 450 to 690 nm in the fundamental, a range that for the RILIS dye laser would require 12 different dyes.

Operating at only 10 Hz, the laser repetition rate at LARIS is lower than that of the RILIS system (10 kHz), where a high repetition rate is required for a good overall ionization efficiency. The difference in repetition rate is therefore prohibitive in terms studying absolute RILIS ionization scheme efficiencies. Relative efficiency measurements however, which are performed at the LARIS lab to determine the optimal RILIS ionization scheme, have been closely reproduced by the RILIS setup. This is discussed in Section 3.1.

There are two vacuum chambers available for the production of atomic beams for ionization studies. The primary system, which uses a tantalum oven capable of reaching a temperature of 1400°C , is suitable for the ionization studies of most of the stable elements that are released from an ISOLDE target. For elements with a low vapour pressure at this temperature, a second system, which relies on laser ablation for sample preparation, is used:

3.0.0.5 Thermal Source

The chamber housing the thermal source is a standard six-way cross design. A cylindrical resistively heated tantalum oven is mounted horizontally and attached to the chamber with a water cooled flange. This can be loaded with a sample (some mg) and heated to a maximum of 1400°C using a 220 A (15 V) DC power supply. A temperature versus electrical current calibration, performed using an optical pyrometer, is used to estimate the oven temperature. The oven, which is 30 mm long and has an internal diameter of 3 mm, produces a low divergence atomic beam which traverses the vacuum chamber to cross the laser interaction point at a distance of approximately 15 cm from the oven exit. Two 7 mm circular aperture electrodes positioned 30 mm from the oven output enable suppression of surface ions as well as geometrically restricting the emerging atom beam. The laser beams enter the chamber through a UV grade fused silica window and converge, normal to the atom beam at the center of the chamber. The beams exit the chamber through a second window and are stopped by an observation screen or a power meter. At the laser/atom interaction point, the diameter of the atomic beam is estimated to be 30 mm and the laser beams are between 3 mm and 7 mm in diameter. The vacuum pressure is typically $<10^{-6}$ mbar at the interaction point. There are two ion detection units available, either of which can be mounted on the top of the chamber, directly above the interaction region. The first system, which was used for the manganese measurements described in Section 3.1, is a simple ion deflector unit which directs the laser produced ions towards a *Del Mar Photonics MA34/2* double micro-channel plate (MCP) detector. The MCP has an effective detector diameter of 25 mm, a typical gain of $10^6 - 10^7$ and a response time of <1 ns. With a large detector surface and many detection channels, this system has a high detection efficiency and a large dynamic range, making it ideally suited to fast, wide range exploratory laser scans where the ability to resolve individual isotope components of the ion signal is not required. For more meticulous measurements, particularly those for which isotope resolution or low background is important, a second system, comprising of a time of flight mass spectrometer (TOF-MS) and electron multiplier detector is used. This is a commercial unit from *KORE Technology Ltd.* and houses a reflectron type TOF-MS within a high vacuum chamber ($<10^{-8}$ mbar). An electrostatic transfer lens focuses the ion bunch through the differential pumping aperture where its trajectory can be manually adjusted via orthogonal deflector plates for alignment through the TOF tube and back towards the entry aperture of a discrete dynode electron multiplier. A mass resolving power ($M/\Delta M$) of up to 200 is achieved.

3.0.0.6 Ablation Source

For the study of refractory metals, a Smalley type [7] laser ablation chamber and TOF-MS, built at Stockholm University is used. A detailed description of this apparatus is provided by Ref. [8]. For this system, the 532 nm output of a *New Wave Research Inc. Polaris III* Nd:YAG laser (operating at 10 Hz with a variable pulse energy from 0 - 50 mJ) is focused onto a rotating rod target to produce an atomic plume by laser ablation. The rod is interchangeable and serves as either a solid sample itself, a metal substrate for a coating containing the sample, or a rigid support onto which a thin foil of the metal of interest can be attached. Argon is injected into the ablation region by a pulsed gas valve which is synchronized with the laser ablation pulse. The atomic sample and the carrier gas expand freely into the first vacuum chamber (10^{-4} mbar). A skimmer separates this chamber from a second, higher vacuum (10^{-6} mbar) ionization region. The atom beam emerging from the skimmer is well collimated and crosses the laser beam at normal incidence. Acceleration and deflection plates ensure that photo-ions created enter the a 1.2 m reflectron TOF-MS tube and the reflected ions are incident upon a dual MCP assembly and a mass resolution of greater than 200 is possible. This system was originally designed for the study of clusters by laser spectroscopy, for which the cooling (down to a few Kelvin) of the sample resulting from the fast expansion of the carrier gas into the high vacuum region, is an essential feature. For resonance ionization spectroscopy of atoms however, a more simple system whereby laser spectroscopy is performed directly on the ablation plume is commonly used [9]. The primary advantage of Smalley type source for this application is that, due to collisions with the high density carrier gas, a greater proportion of the sample

Table 3: LARIS tunable laser specifications

Laser (operating at 10 Hz)	Wavelength range		Pulse duration (ns)	Pulse energy (mJ)	Linewidth (GHz)
	min (nm)	max (nm)			
SP MOPO-HF signal	450	690	8	70 @500 nm	10
SP Signal FDO	220	345	10	7.5 @250 nm	14
SP MOPO-HF idler	750	1680	8	35 @800 nm	10
SP Idler FDO	375	450	10	3 @400 nm	14
Continuum Mirage OPO	720	920	6	80 @750 nm	2
Continuum Mirage FDO	365	450	7	10 @425 nm	3
Lumonics HyperDye	550	850	6	30 @600 nm	5
Lumonics FDO	275	425	8	5 @300 nm	7

is in the atomic ground state when it reaches the laser interaction region.

Table 3 lists the main characteristics of the LARIS tunable lasers. The accessible spectral range covers the combined output range of Nd:YAG pumped dye lasers and Ti:Sapphire lasers. If non-resonant ionization is required, either the *Polaris III* ablation laser, or the Lumonics HyperDye pump laser (a *Quantel Brilliant* Nd:YAG) can be used. In standard operation, the 532 nm output of the *Quantel* laser is used but it can be equipped with third, fourth or fifth harmonic generation modules if necessary. The laser system is synchronized with low jitter (<2 ns) using a *Thales Masterclock* and two *Stanford Research DG535* digital delay generators.

During acquisition mode, a *Laser2000 LM007-UV* wavemeter is used to measure the wavelength of the scanning laser. A computer running a *LabVIEW* based data acquisition system records these values after performing a filtering algorithm to accept only measurements within a defined range and tolerance. This ensures that no ion counting occurs when the laser is either between scanning steps or has become unstable. Provided that an acceptable wavelength reading is available, the program records this together with a corresponding output parameter from a *LeCroy Waverunner 104MXi* Digital Sampling Oscilloscope (DSO). In most cases this parameter is the integral of the detector signal within one or more time gates, which correspond to ion bunch arrival windows at the MCP or electron multiplier detector. Up to 8 parameters from the DSO can be recorded during the acquisition cycle and since the laser repetition rate is low, the acquisition suffers no duty cycle losses. The wavelength and DSO parameters can be recorded alongside power or energy measurements of up to three lasers through the use of *OPHIR* power meters which communicate with *LabVIEW* through the *NI-VISA* interface. If a pyroelectric energy sensor is used, the pulse energy for each laser shot can be measured, therefore enabling a post acquisition analysis of the ion production that results from each laser pulse. Since this is a passive system which does not communicate with the laser but relies only on a valid wavemeter reading to begin the acquisition process, it performs equally well regardless of which laser is used for scanning.

3.1 New ionization scheme for manganese

The CVL pumped RILIS ionization scheme for manganese was developed at ISOLDE in 1996 [10]. That work involved the testing of 9 three-step ionization schemes with each scheme using both the green and yellow CVL beams for ionization. Three first-step transitions were used and from each first excited state, transitions to three different second excited states were studied. The relative efficiency of each scheme was measured and for each resonant transition a saturation measurement was performed. The 6 strong transitions to two of the second excited states were saturated but an unexpected observation was that the optimal scheme, shown on the left hand side of Fig. 1 uses a weak second step transition ($\lambda = 628.44$ nm; $\log_{g,f} = -3.044$ [11]) which is not saturated. The conclusion, which was verified by a comparison of

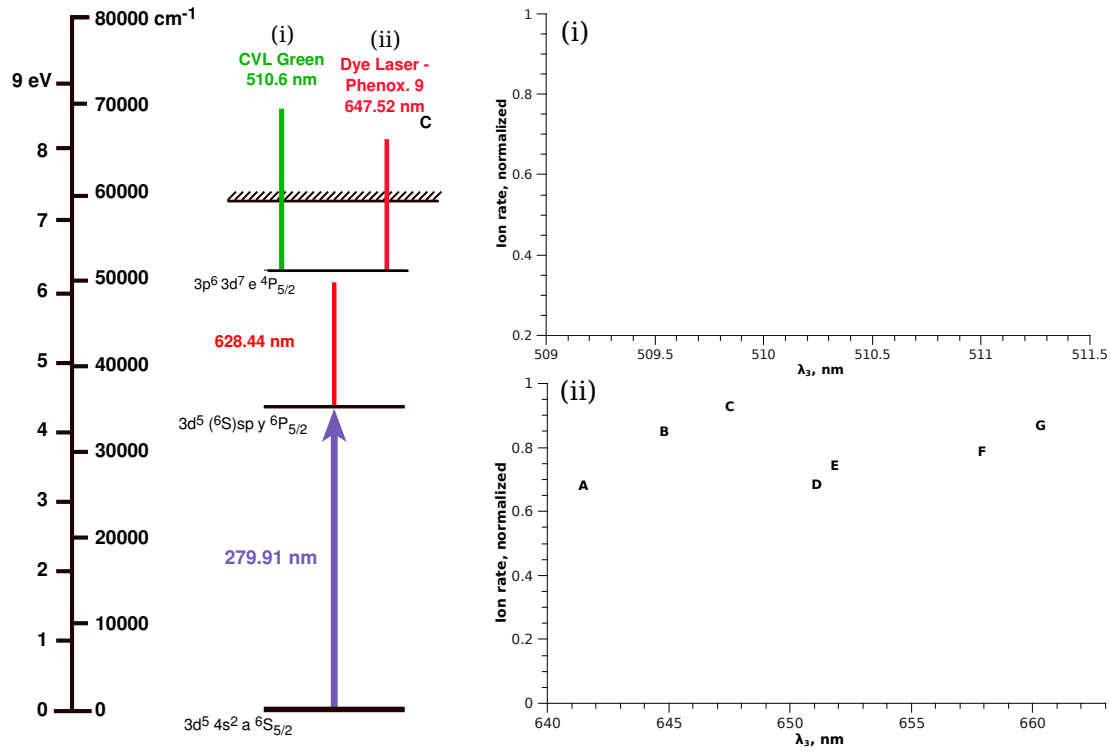


Fig. 1: The CVL based RILIS scheme shown alongside the newly developed Nd:YAG pumped RILIS scheme. Plot (i) shows the auto-ionizing state reached by the green CVL beam. Plot (ii) shows a laser scan covering several of the auto-ionizing states that are within the range of the Phenoxazone 9 laser dye

the ion rate enhancement provided by CVL green and yellow beams, was that the third step transition using the green beam was to an auto-ionization state.

Plot (i) in Fig. 1 is part of a fast broadband scan of the ionization continuum of manganese performed at the LARIS lab using the signal beam of SP-MOPO laser as the third step of the RILIS ionization scheme. Here it is seen that the green CVL beam (510.56 nm) does indeed reach a broad multiplet of auto-ionization states centered around 71219.14 cm^{-1} (510.7 nm). Unsurprisingly, a continuation of this scan to longer wavelengths showed no auto-ionization state coinciding with the 532 nm output of the Nd:YAG laser. A resonance ionization spectroscopy study of manganese was therefore conducted with the aim of determining an optimal ionization scheme for RILIS with Nd:YAG pumping. The extent of this study, for which all three LARIS tunable lasers (Table 3) were required, is shown in Fig. 2. The thermal atomic beam source, loaded with a small quantity (some mg) of manganese shavings was used and ion detection was performed with the MCP detector unit. A temperature of approximately 600°C was reached with a heating current of 80 A and ensured a stable long term (over 5 hour) release of manganese vapour.

Since the achievable pulse energy of the LARIS lasers is typically 100 times greater than can be generated by the RILIS laser system, care must usually be taken to ensure that the laser powers required for an ionization scheme are not unrealistic for application at RILIS. For manganese however, this was not a primary concern since the RILIS performance for transitions to the intermediate excited levels has been well documented [10]. Instead, an excess of pulse energy was beneficial since a strong saturation of these transitions was effective in minimizing the ion count rate fluctuations due to power or laser frequency instabilities. The pulse energies used for the first and second steps were $10 \mu\text{J}$ and $600 \mu\text{J}$

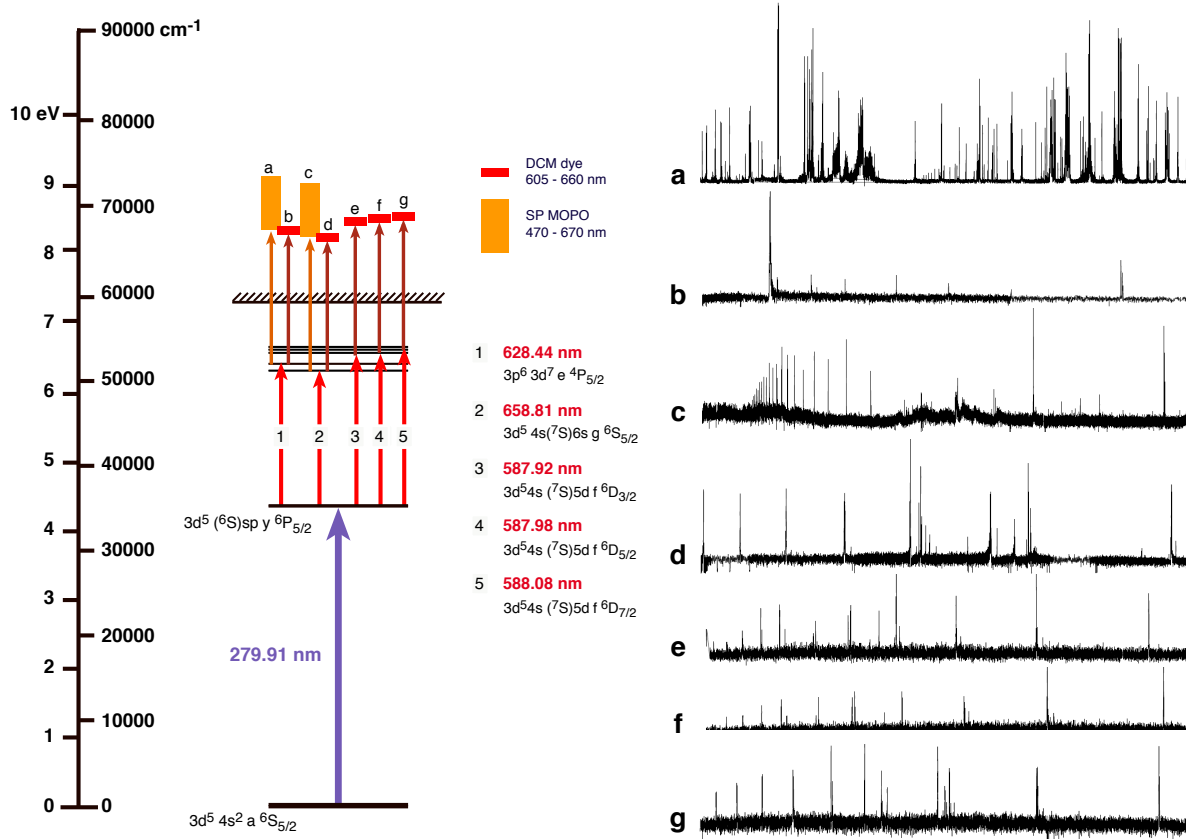


Fig. 2: The extent of the spectroscopy of manganese performed at the LARIS Laboratory. The plots show photoion rates versus laser wavelength for the laser scans shown in the figure: Plots **a** and **c** show a range of 470-670 nm; plots **b**, **d**, **e**, **f** and **g** show a range of 605-660 nm

respectively. For performing scans with the third step laser two modes of operation were used: Fast, wide-range, continuous scanning at high power and slow, incremental scanning at reduced power. In fast-scan mode the pulse energy was high (1-5 mJ) to ensure that strong resonances are broadened and therefore easily detectable with a scanning rate of 0.02 nm/s. The data in Plot (i) of Fig. 1 and in the spectra displayed in Fig. 2 were obtained in this mode. Slower (0.005 nm/s) scans with reduced pulse energy were performed as repeat measurements over selected regions of interest. Plot (ii) of Fig. 1 is an example the data obtained in this mode.

As shown in Fig. 2 the ionization continuum of manganese was probed using five different pump schemes, each using the same first step transition. Many auto-ionizing states were identified but the majority were observed only as transitions from the mixed configuration level at 51638.17 cm^{-1} . Some of the strongest of these lie within the Phenoxazone-9 dye tuning range and were measured at RILIS during the preparation for a scheduled manganese beamtime. The ion currents obtained for the stable ^{55}Mg isotope for the 7 ionization schemes that were measured are shown in Table 4. Fig. 3 illustrates the degree of agreement between the relative ionization scheme efficiencies measured at RILIS and LARIS respectively. The discrepancy between these values for schemes F and G can be accounted for by the loss of output power of the RILIS dye laser as the upper limit of the dye tuning range is approached.

4 Conclusion

The *Edgewave* Nd:YAG pump laser has proven to be a suitable replacement for the CVL system. Operational benefits such as a short start-up and shutdown times and a reduction in the maintenance workload

Table 4: Auto-ionizing levels which were observed at both LARIS and RILIS. The relative efficiencies of schemes using these transitions are shown in Fig. 3.

$\lambda_2(\text{vac})$	$E_2 (\text{cm}^{-1})$	Configuration [12]	$\lambda_3(\text{vac})$	$E_3 (\text{cm}^{-1})$	Ion current [†] , pA	Label [‡]
628.44	51638.17	$3p^6 3d^7 e^4 P_{5/2}$: 90%	641.45	67227.9	310	A
628.44	51638.17	$3p^6 3d^7 e^4 P_{5/2}$: 90%	644.77	67147.5	350	B
628.44	51638.17	$3p^6 3d^7 e^4 P_{5/2}$: 90%	647.52	67081.7	400	C
628.44	51638.17	$3p^6 3d^7 e^4 P_{5/2}$: 90%	651.15	66995.7	350	D
628.44	51638.17	$3p^6 3d^7 e^4 P_{5/2}$: 90%	651.78	66980.7	310	E
628.44	51638.17	$3p^6 3d^7 e^4 P_{5/2}$: 90%	657.93	66837.4	230	F
628.44	51638.17	$3p^6 3d^7 e^4 P_{5/2}$: 90%	660.31	66782.5	300	G
658.81	50904.68	$3d^5 4s(^7S)6s g^6 S_{5/2}$	617.43	67101.9	220	H

$$\lambda_1(\text{vac}) = 279.91 \text{ nm}; E_1 = 35725.85 \text{ cm}^{-1}$$

[†]Measured at RILIS

[‡]The labels correspond to the the markers used in Fig. 1 and Fig. 3

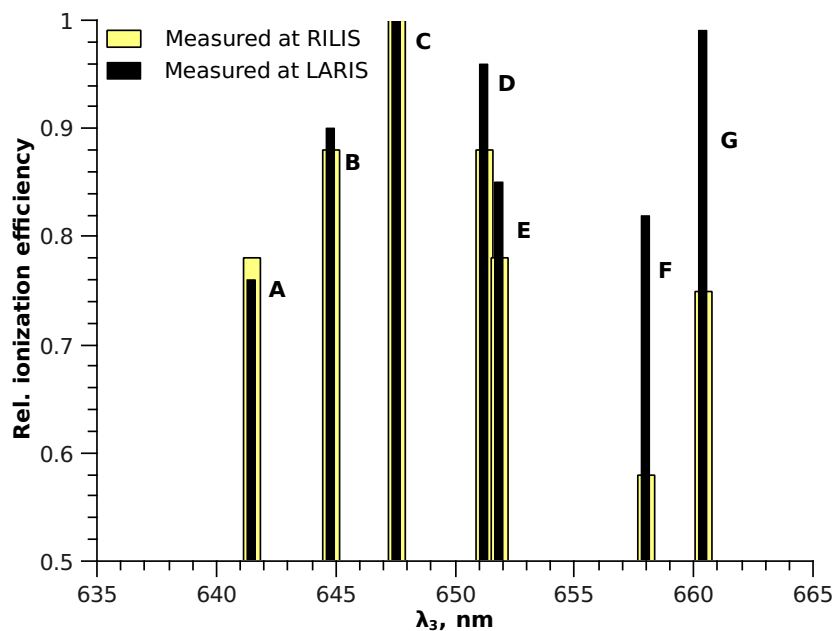


Fig. 3: Comparison of the relative efficiencies of the schemes described in Table 3 measured at both RILIS and LARIS

have been welcomed. All users of the RILIS ionized ion beams benefit from the improved laser power stability and reliability. The higher output power has resulted in an improvement in the ionization efficiency for many elements. The successful application of an alternative ionization scheme for manganese has verified the reliability of the LARIS studies to determine the optimal RILIS ionization scheme. The LARIS work program, which focuses on improving the performance of the Nd:YAG pumped RILIS ionization schemes, is ongoing.

Acknowledgements

Funding for the RILIS pump laser upgrade and the LARIS laboratory was provided by a grant (KAW 2005-0121) from the Knut and Alice Wallenberg Foundation (Sweden). This work was performed with support of the European Union Sixth Framework through RII3-EURONS Contract No.506065.

References

- [1] Mishin, V., Fedoseyev, V., Kluge, H.-J., Letokhov, V., Ravn, H., Scheerer, V., Shirakabe, Y., Sundell, S., Tengblad, O.: Nucl. Instrum. Met. Phys. Res. **B 73**, 550 (1993)
- [2] Fedoseyev, V., Huber, G., Köster, U., Lettry, J., Mishin, V., Ravn, H., Sebastian, V.: Hyperfine Interact. **127**, 409 (2000)
- [3] Lindroos, M., Butler, P., Huyse, M., Riisager, K.: Nucl. Instrum. Met. Phys. Res. **B 266** (19-20), 4687 (2008)
- [4] Fedosseev, V., Berg, L., Lebas, N., Launila, O., Lindroos, M., Losito, R., Marsh, B., Osterdahl, F., Pauchard, T., Transtromer, G.: Nucl. Instrum. Met. Phys. Res. **B 266** (19-20), 4378 (2008)
- [5] Du, K., Wu, N., Xu J., Giesekus, J., Loosen, P., Poprawe, R.: Optics Letters. **23** (5), 370 (1998)
- [6] Marsh, B. A., Fedosseev, V. N., Kosuri, P.: Hyperfine Interact. **171**, 109 (2007)
- [7] Smalley, R. E.: Laser Chem. **2** (3-4), 167 (1983)
- [8] Doverstal, M., Lindgren, B., Sassenberg, U., Yu, H.: Physica Scripta **43**, 572 (1991)
- [9] Gangrsky, Yu. P., Zemlyanoi, S. G., Izosimov, I. N., Markov, B. N., Tam, T. K.: Instruments and Experimental Techniques, **33**, 168 (1990)
- [10] Batzner, K., Fedoseyev, V.N., Catherall, R., Evensen, A.H.M., Forkel-Wirth, D., Jonsson, O.C., Kugler, E., Lettry, J., Mishin, V.I., Ravn, H.L., Weyer, G.: Nucl. Instrum. Met. Phys. Res. **B 126** (1-4), 88 (1997)
- [11] Kurucz, R.: Transactions of the International Astronomical Union, Volume XXB. (ed. M. McNally), Kluwer, Dordrecht) pp. 168-172 (1988)
- [12] Ralchenko, Y., Kramida, A.E., Reader, J., and NIST ASD Team: NIST Atomic Spectra Database **3.1.5**, (2008)